# DYNAMIC CRACK INITIATION IN THE STEEL 20MnMoNi 5 5

R.Clos, U. Schreppel, P. Veit and U. Zencker*

The crack initiation in fine grained steel 20 MnMoNi 5 5 has been investigated under stress wave loading conditions in the temperature range from - 50 °C up to 20 °C by a loading setup similar the "Split Hopkinson Pressure Bar" technique. For temperature up to 20 °C fracture occurs by cleavage and $K_{Id}$ approaches and falls below the reference fracture toughness, while at room temperature stable crack growth occurs with a $J_i$ close to the static initiation value of the J-integral. The analysis of the crack tip configuration suggests that the stable crack growth is the result of the following simultaneously induced stochastical processes: generation of constrained local microcracks, blunting of the individual crack tips and the deformation of material bridges at different regions along the crack tip front.

## EXPERIMENTAL METHODS

The loading setup is shown in Fig. 1a. It consists essentially of a gas gun, a long input bar (circular cross section, diameter 20 mm, length about 1 m) and the fatigue precracked specimen. The specimen is pressed slightly against the bar in such a way, that its right end can be considered as a free end within the investigated time range. By the impact of the projectile a pressure pulse of short duration is generated in the input bar. The pulse propagates through the bar and the specimen. At the free end of specimen it is reflected as a tensile pulse, which interacts with the crack and can cause crack propagation depending on its amplitude. Usually a finite amount of crack growth is produced. The pulse is measured with a coaxial capacitive gauge and recorded with a digital oscilloscope (the time resolution is usually 0.1 $\mu$s). With this type of stress wave loading crack tip loading rates $K_I$ up to $10^7$ MPam$^{1/2}$/s can be attained (1).

* Otto von Guericke Universität Magdeburg, Institut für Experimentelle Physik
Universitätsplatz 2, 39106 Magdeburg, Germany.

The structure and configuration of cracks in the precracked and stress pulse loaded specimen were studied by light microscopy. For this purpose the specimens were cutted into slices (Fig. 1b). The 3D - crack profile was reconstructed by carefully step by step sectioning parallel to the x - y plane with a step size of $\Delta z \approx 4\ \mu m$. The density and arrangement of the precipitates and dislocations were studied by transmission electron microscopy quantitatively. Some of the loaded specimens (with finite crack growth) were finally fractured in liquid nitrogen and the fracture surfaces were investigated by scanning electron microscopy. The quantitative analysis was carried out with a digital image analysis system. The J-integral versus time curves and the development of the plastic zone at the stress pulse loaded crack tip were determined by 3D- FE/FD- calculations (Fig. 2). Details of the experimental methods are given in (2).

## RESULTS AND DISCUSSION

The investigated material is a bainitic-martensitic steel (grain size 8 $\mu$m) with a small content of ferrite (grain size 16 $\mu$m) and banded structure. Nearly globular carbides were found along the grain boundaries (about 0.2 $\mu$m in diameter) and within the boundaries (about 30 nm in diameter). The original microstructure is dominated by dislocation cells.

A typical fatigue crack path is shown in fig. 3. The freguency and length of the secondary microcracks are influenced by the morphology of grains.

The fracture behaviour in the applied loading rate range from $5 \cdot 10^6$ up to $10^7$MPam$^{1/2}$/s indicates a strong temperature dependence. For temperatures up to 20 °C crack propagation occurs by cleavage (see fig. 4) and the dynamic fracture toughness $K_{Id}$ approaches and falls below the reference fracture toughness ($K_{IR}$ -curve in fig. 5). In the temperature range from -50 °C up to -35 °C the fracture toughness is insignificantly above the static values. The mechanism of crack propagation is dominated by cleavage connected with fields of microcracks around the propagated crack tip (see fig. 3).

Above -20 °C the crack propagation is dominated by ductile fracture initiation on a macroscopic scale.

The results of the quantitive metallography and fractography at the loading temperature 20 °C (fig. 6) show that already at low pulse stresses a rugged crack front (see fig. 7) is formed. The microscopic crack growth mechanism at increasing J-integral consists of the following successively and simultaneously occuring processes:

i) Generation of isolated small microcracks along the front of the mean crack. The probability of generation as well as the area and direction of microcracks depend on the local microstructure. Material bridges (ligament) between these "structural" microcracks hinder the growth of the microcracks (constrained growth, $J_i^e$ in fig. 8).

ii) Plastic deformation of the material bridges and blunting of the individual crack tips. This process dissipates energy and the work hardening inside the plastic zone increases the yield stress.

iii) Ductile fracture of the ligament between the blunted microcracks. The large plastic strains developed ahead of the crack tip initiate necking. Nucleation, growth and coalescence of microvoids during necking generate small dimple bands.

A temporarily closed crack front is necessary for macoscopic crack intiation. It is important to note that under the applied loading conditions isolated voids or microcracks were not observed.

Based on the quantitative microscopical investigation an initiation value $J_i$ of 160 N/mm has been calculated, which is only insignificantly above the static initiation value of the J- Integral (fig. 8).

Due to the highly transient loading with rise times in the order of 10 $\mu$s the commonly used constitutive equations (e.g. viscoplasticity according to Prezyna, Bodner-Partom) are not suited for the numerical simulations. Especially the strong loading rate dependence of the upper yield point has to be taken into account. This has a pronounced effect on the development of the plastic zone at the crack tip. In this way it was found a good agreement between the FE- calculations of plastic deformation around the loaded crack tip (fig. 2) and recrystallisation experiments.

## REFERENCE

(1) Stroppe, H.. R. Clos and U.Schreppel, Nuclear Engineering and Design Vol. 137, 1992, pp. 315- 321.

(2) Clos,R."Rißverhalten bei Spannungswellenbelastung", BMFT-Report No. 1500 851, 1993.

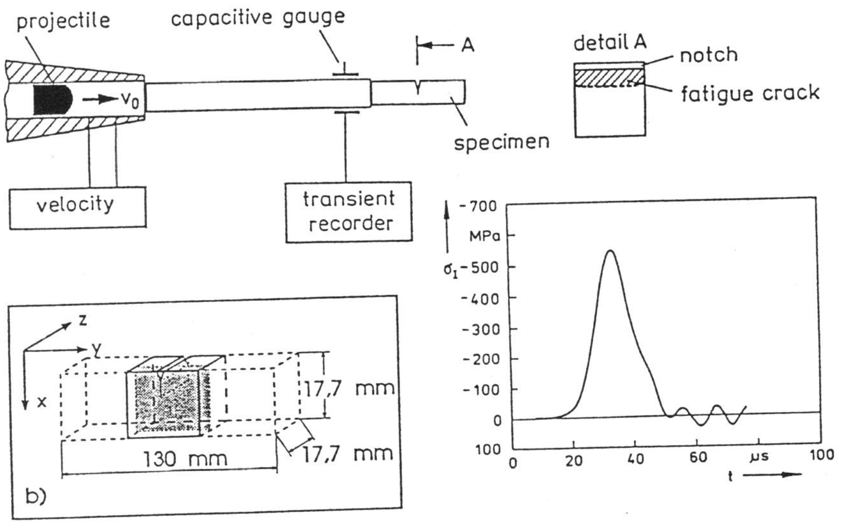

Figure 1 Pulse loading setup (a), size of specimen and preparation coordinate system (b) schematically

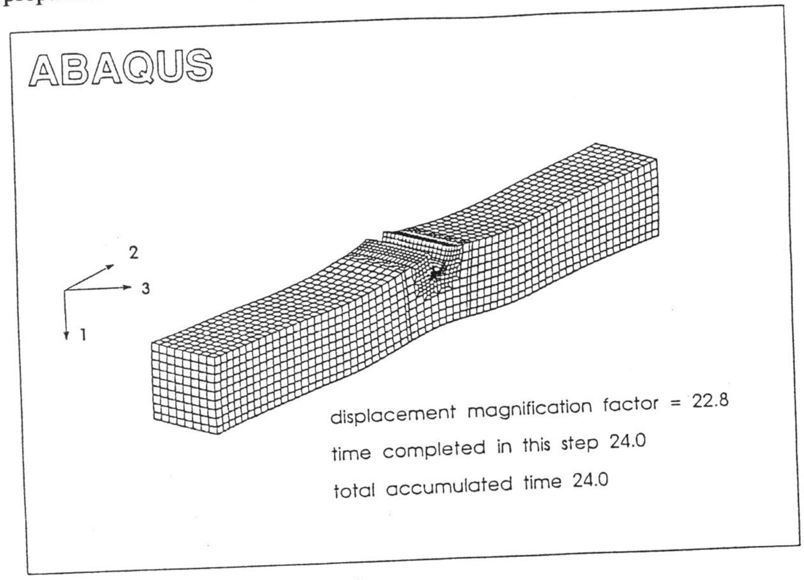

Figure 2 Loaded 3D - FE specimen

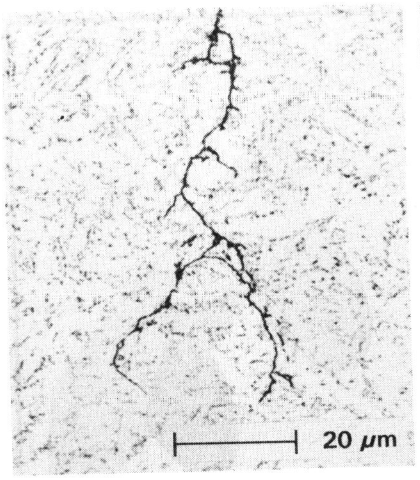

Figure 3 Micrograph of a typical fatigue crack tip

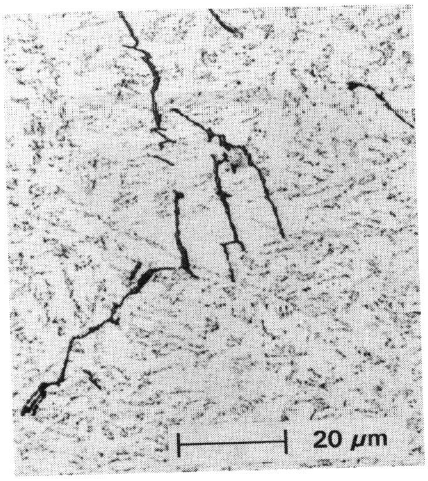

Figure 4 Ensemble of microcracks

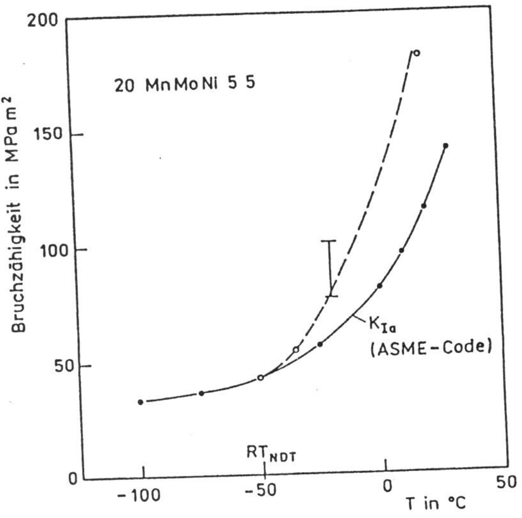

Figure 5 Fracture toughness vs. temperature

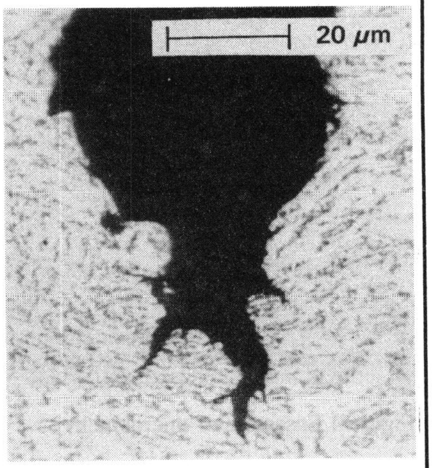

Figure 6 Micrograph shows the blunting effect

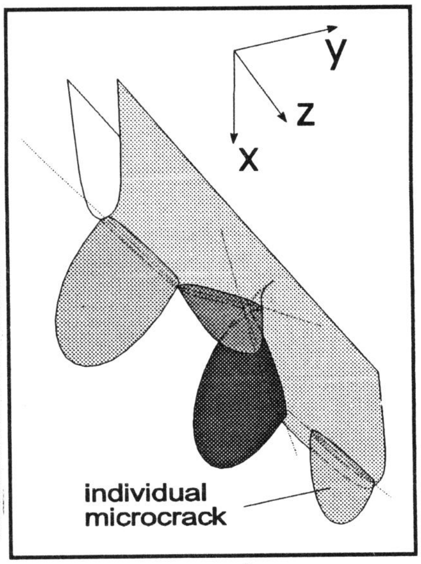

Figure 7 3D- reconstruction of crack front schematically

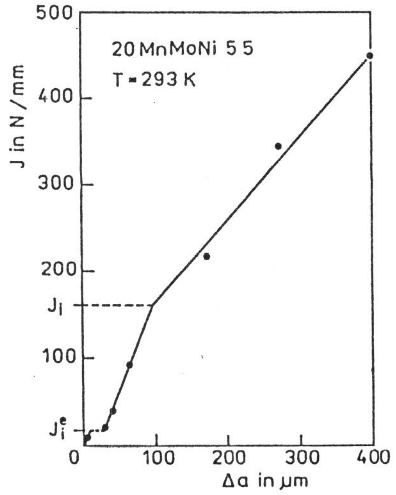

Figure 8 J - Δa curve